URadio: Wideband Ultrasound Communication for Smart Home Applications

Qiben Yan, Senior Member, IEEE, Qi Xia, Yuanda Wang, Pan Zhou, Senior Member, IEEE, Huacheng Zeng, Senior Member, IEEE

Abstract—Smart home Internet-of-Things (IoT) has a vibrant market with a wide range of appliances and sensors, spanning across smart home, smart city, and smart factory. However, the security and privacy of these IoT systems have raised serious concerns. Currently, most IoT devices rely on electromagnetic wave-based radio frequency (RF) for communication. Yet, RF has several inherent limitations such as shortage of spectrum, susceptible to interference, and vulnerable to eavesdropping or jamming attacks. This paper presents URadio, a wideband ultrasonic communication system. By leveraging recent advances in reduced Graphene Oxide (rGO), we design a new type of electrostatic ultrasonic transducer, which can achieve more than 6× bandwidth than commercial ultrasonic transducers. With this new transducer, we design an OFDM communication system to maximize its data rate for smart home applications. We build a prototype of URadio on a wireless testbed and evaluate its performance in several real-world environments. Our experiments show that URadio can reach up to 360 kbps data rate at a distance of 81 cm or 20 kbps data rate at a distance of 20 m, which supports a variety of smart home applications. We further showcase URadio's resilience against eavesdropping and jamming attacks, as well as demonstrate its capability of securely localizing objects in an indoor environment.

Index Terms—Ultrasonic communication, smart home, eavesdropping, indoor localization.

I. INTRODUCTION

Smart home Internet-of-Things (IoT) has experienced a tremendous growth in recent years. Home automation systems, such as Samsung SmartThings, Google Home, Apple Homekit, and Amazon Alexa, which provide infrastructure and services to exchange all types of appliance information and data, have become increasingly intelligent and sophisticated. Radio Frequency (RF) based communication protocols, such as WiFi, Bluetooth, Zigbee, and Z-wave, are widely used to connect IoT devices. However, since data is transmitted in the form of RF signals, IoT devices are inherently susceptible to the common physical-layer attacks towards wireless networks, including radio jamming [1], eavesdropping [2], signal manipulation [3], etc.

Airborne ultrasonic radio has recently aroused some interests due to its multi-faceted advantages over traditional

This work was supported in part by NSF under Grant CNS-1950171 and Grant CNS-1949753. Pan Zhou is funded by the National Natural Science Foundation of China (NSFC) with grant numbers 61972448. (Corresponding author: Qiben Yan)

RF systems. Specifically, RF communication suffers from strict regulation, severe interference entangled with increasing number of devices, and aggravated security concerns in an adverse environment. Ultrasonic communication, on the other hand, operates within any acoustic frequency bands in a mostly interference-free environment. Meanwhile, there is currently no regulation on ultrasound spectrum usage. Compared with RF signals, ultrasonic signals have a miniature footprint, which makes it difficult to intercept, as highly-directional ultrasonic signals can only transmit effectively over the line of sight (LoS) links, and could hardly penetrate through solid walls [4]. These salient features of ultrasonic communication greatly reduce its exposure risks to the eavesdroppers and jammers. As a result, ultrasonic radio is complementary to its RF counterpart, especially when high-standard communication security is required or strong electromagnetic shields exist. However, airborne ultrasonic communication suffers from limited bandwidth due to the severe propagation loss of ultrasound and the limited bandwidth offered by existing commercial ultrasonic transducers.

Recent studies have investigated airborne ultrasonic data transmission with real system implementations. For example, a wearable ultrasonic communication system, U-Wear [5], achieves a data rate of 2.76 kbps using Gaussian Minimum Shift Keying (GMSK) modulation. Another ultrasonic communication system [6] has been developed to exploit the nonlinearity property of the microphone's membrane to transform an ultrasonic signal into an audible signal, which achieves a data rate of 4 kbps. Chirp and Multiple Frequency-Shift Keying (MFSK) modulation have also been used to transmit inaudible signals at 16 bps and 800 bps, respectively [7], [8]. These low data rate transmission systems meet the demands of some IoT applications with intermittent data exchanges, such as text messaging, command-and-control, cross-device tracking, and targeted advertising [9]. However, a large quantity of modern smart home applications require a higher data rate, including online picture browsing, large file sharing, and video streaming. Yet, designing a high-speed ultrasonic communication system is particularly challenging due to the lack of a wideband transducer.

In an acoustic transducer such as a mobile microphone, air pressure variations from a sound wave induce motion of a suspended diaphragm, which is in turn converted into an electrical signal. The key to achieve wideband ultrasonic communication is a *lightweight diaphragm* for sound generation/detection. Thinner and lighter diaphragms can lead to more faithful tracking of sound vibration at the higher frequencies. The

1

Q. Yan, Y. Wang, H. Zeng are with the Department of Computer Science and Engineering, Michigan State University, East Lansing, MI 48824, USA (e-mail: qyan@msu.edu).

Q. Xia is with with the Department of Electrical and Computer Engineering, University of Texas San Antonio, San Antonio, TX, USA. P. Zhou is with Huazhong University of Science and Technology.

recent advancement shows that Graphene, only one-atom thick (0.33 nm) but mechanically strong, can be used to construct the ultra-lightweight diaphragms [10]. However, Graphene diaphragms are extremely brittle and easy to be fractured [10]. In contrast, reduced Graphene Oxide (rGO), an oxidized product of graphite, has sufficient strength while preserving the thinness [11]. Meanwhile, rGO membranes can be easily fabricated, mechanically robust, and amenable to industrial-scale production with a low cost [12], hence, they could be suitable for designing wider-bandwidth ultrasonic transducers.

In this paper, we present URadio, a wideband ultrasonic radio system equipped with two types of transducers, including one commercial-off-the-shelf (COTS) transducer and one lab-made transducer, which is made of rGO membrane measured at 0.4 μ m thick. We design an electrostatic ultrasonic transducer structure integrated with the membranes to achieve the highest vibration and reception sensitivity. URadio implements the OFDM modulation to better utilize the wide bandwidth that is achieved by the newly designed transducers. We thoroughly test the URadio system, and show the high speed, efficiency, and secure communication of the proposed system. Finally, to test its real-world applicability, we develop and evaluate an ultrasound-based object localization application on top of URadio.

Application scenarios. Popular smart home devices, such as Google Nest [13], Amazon Echo [14], have incorporated ultrasound transducers for occupancy, user movement detection, and object localization. With a more secure and resilient communication channel, the ultrasonic communication can replace the RF communication using, e.g. Bluetooth, in some high security scenarios. For instance, the communication between digital devices and smart locks carries important secret key information, which can be transferred via ultrasound. Ultrasound communication can also be used to securely deliver important documents among smart devices, such as financial documents, medical records, legal identification documents, etc. Moreover, with the support of wide bandwidth, private video footage can be exchanged between different smart home devices through ultrasound to improve security and user experience. For example, live sleeping footage from a private bedroom can be sent to a sleep tracker securely through ultrasound for sleep disorder diagnosis.

The contributions of this paper are summarized as follows.

- For the first time, we introduce a rGO transducer for IoT applications in smart home. We design a new ultrasound communication system, URadio, which maximizes its data rate by fully utilizing the available bandwidth of both the custom-made and COTS transducers.
- We have built a prototype of URadio and compared its performance with the state-of-the-art systems. Specifically, equipped with COTS transducer, URadio can achieve a communication range of 20.9 m at 20 kbps, while an integrated system with the rGO transducer achieves a range of 81 cm at 360 kbps.
- We further showcase the system's resistance against jamming and eavesdropping attacks, and demonstrate its capability in the domain of object localization in a smart home scenario.

Organization - This paper will be organized as follows: Section II illustrates the background of ultrasonic communication and threat model. Section III presents the design of URadio system, followed by the experimental evaluation in Section IV. Section V demonstrates the object localization application using URadio. Section VI discusses the related work, and Section VII concludes this work.

II. AIRBORNE ULTRASONIC COMMUNICATION

A. Ultrasonic Communication Background

Ultrasonic signals consist of longitudinal mechanical waves propagating in elastic media (e.g., air) with frequency above 20 kHz. Similar to RF signals, two main factors contribute to ultrasound's attenuation over the air: *path loss* and *absorption*. The former includes free-space loss, refraction, diffraction, reflection, and aperture-medium coupling [15], while the latter factor denotes the absorption of ultrasound waves in the air, the impact of which largely depends on the temperature, pressure, and moisture [16]. Since acoustic wave is one type of mechanical wave, it shows significant directionality, weak penetration, and rapid attenuation. As a result, it is more suitable for high security and short-distance applications than the RF wave technology.

Air-coupled ultrasonic transducers. Ultrasonic transducers serve as converters to transform sound wave into electrical current (or vice versa). Nowadays, they can be categorized into two main classes based on their physical mechanisms, i.e. *piezoelectric* and *electrostatic transducers*. In the URadio system, we use electrostatic transducers since they have a wider communication bandwidth compared with piezoelectric transducers, thereby supporting higher data rates.

B. Physical-Layer Threat Model

Smart home technologies rely on the instantaneous and reliable communication between IoT devices. However, RFbased IoT devices are susceptible to a magnitude of physicallayer attacks due to the physical properties of the RF signals. These attacks can be categorized into passive attacks and active attacks [17]. The passive attackers can utilize the widespreading property of RF signals to passively collect the transferring information without being detected, i.e., launching wireless eavesdropping attacks. An active attacker may attempt to alter system resources or disrupt its normal operation by injecting RF signals to the receivers. Active attacks include replay, message modification (man-in-the-middle), denial of service (DoS) or jamming, etc. Although countermeasures exist at upper layers to ensure confidentiality, integrity, and availability, the physical-layer security threats are difficult to eliminate.

In particular, the eavesdropping attacks pose serious threats to a smart home in the presence of insider adversaries that have access to encryption keys. Meanwhile, the jamming attacks could disrupt the communications between devices and cause the denial of service inside a smart home. Moreover, both the replay attack and man-in-the-middle attack require the eavesdropping of exchanged messages between the transmitter and

receiver. Therefore, in this research, we consider leveraging ultrasound to mitigate the two major physical-layer attacks in smart homes, i.e., eavesdropping and jamming attacks. More specifically, the proposed ultrasonic communication channel will serve as an alternative channel to complement the existing RF-based systems in high-security applications. We assume the transmitter and receiver have a direct LoS path, while the attackers (i.e., eavesdropper and jammer) are not on the LoS path. We consider this attack assumption reasonable, since any intruders along the LoS path can be easily spotted and detected. In this work, we also consider that both the transmitter and receiver are at fixed positions. Note that the security of upper-layer cryptographic protocols and physical device capturing threats are out of the scope of this work.

C. Problem Formulation

Leveraging an ultrasound based communication channel, the devices would be much less vulnerable to the above-mentioned security threats. Compared with RF signals, ultrasonic signals could barely penetrate through solid materials such as doors and walls and attenuate faster over the air. In addition, since jamming and eavesdropping attacks require dispersed wireless signals, an ultrasonic communication system is more physically secure against physical-layer attacks. However, the physical characteristic of ultrasound also limits its available bandwidth when used for ultrasonic communication. To realize high data rate ultrasonic communication, we need to develop a secure ultrasonic system that satisfies the bandwidth requirement. In this paper, we develop a system, URadio, to effectively resolve the conflict between wideband communication and security. Not only does URadio support wideband ultrasonic communication, but it also simultaneously achieves jamming-resilience, and immunity to eavesdropping attackers who are off the LoS path.

III. URADIO SYSTEM DESIGN

The URadio system consists of a set of software and hardware components. Fig. 1 presents the URadio system architecture, in which a waveform generator produces signals to be amplified by a power amplifier. Then, the amplified signals are converted and transmitted as ultrasound signals by the transducer. At the receiver side, the transducer captures ultrasound signals, which will be amplified by a preamplifier and decoded by an oscilloscope.

A. System Overview

As shown in Fig. 1, the URadio system consists of both hardware components and software components. The transmitter and receiver transducers are specially designed to support wideband ultrasound communication with the design details presented in Section III-B. Since the membrane vibration in the ultrasonic transducer only produces very weak electronic signals, both the transmitter and receiver need amplifiers to amplify the signals for signal processing. The design of amplifiers are illustrated in Section III-C. The URadio system software uses the OFDM communication protocol to support the wideband ultrasonic communication. We carefully select

the operational bandwidth of the ultrasonic communication to maintain the orthogonality of OFDM subcarriers, and the synchronization and channel estimation are designed to better support the lower data rate acoustic communication rather than the higher data rate RF communication. At the transmitter side, the OFDM transmitter includes modulation, pilot insertion, IFFT, preamble insertion, up conversation, and linear frequency modulation (LFM). At the receiver side, the OFDM receiver performs signal identification, down conversion, synchronization, FFT, channel estimation, equalization, phase error correction, and demodulation. The details of URadio software design is presented in Section III-D.

B. Transducer Design

Mathematical Model: We design URadio with two different types of transducers, including one COTS transducer (SensComp 600 series [18]), which is shown in Fig. 2, and one lab-made rGO transducer shown in Fig. 3, to achieve long-range and wideband ultrasonic data transmission, respectively.

Formally, the movement of a diaphragm could be modeled as a second-order spring-damping-mass system. The formula that describes the movement of the diaphragm can be written as:

$$F = m\frac{d^2x}{dt^2} + \zeta\frac{dx}{dt} + kx,\tag{1}$$

where x is the displacement of diaphragm, t is the time, t is the mass of diaphragm, t is the damping coefficient, t is the spring constant, and t is the driving force applied onto the diaphragm. When driven by a stimulus sinuous signal at frequency t, the vibration amplitude can be written as:

$$\left| \frac{dx}{dt} \right| = \frac{|F|}{|\zeta + i(2\pi f m - (2\pi f)^{-1} k)|}.$$
 (2)

Here, the vibration amplitude is represented in the form of velocity rather than displacement, because the *sound pressure level (SPL)* is directly determined by the velocity amplitude of air:

$$SPL = c\rho \left| \frac{dx}{dt} \right|,\tag{3}$$

where c is the sound velocity and ρ is the mass density of air. From the above set of equations, we note that a larger mass m results in a poorer high frequency response (i.e., f in Eq. (2)). As a result, the mass density of the diaphragm sets an upper limit on the frequency response of a transducer. It is thus clear that, in order to increase the bandwidth, thinner and lighter diaphragms should be employed for more faithful tracking of sound vibration at higher frequencies.

Fabrication of rGO Transducers: We design and produce the rGO transducers with a 3D printer and the device is displayed in Fig. 3. Briefly, the transducer is built with an rGO membrane $(0.4~\mu m)$ thick) suspended midway between two perforated electrodes, which are constructed by a stainless steel woven mesh sheet. Spacers, which are made of polyethylene terephthalate (PET) sheets, sandwich the membrane and prevent it from touching the electrodes.

In this process, we fabricate two rGO membranes with different gap sizes: rGO-D4G50 and rGO-D4G100, with 50 μ m, 100 μ m gap sizes, respectively, and 4 mm hole diameter. Our measurement indicates that the rGO membrane is

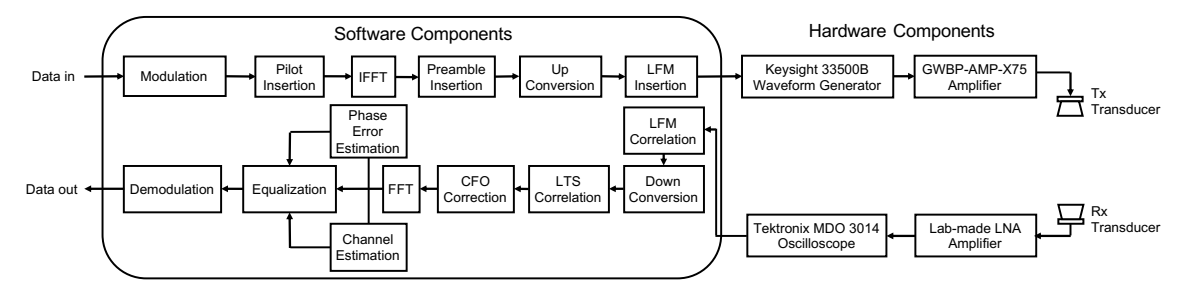


Fig. 1: URadio system architecture.



Fig. 2: SensComp series 600 ultrasonic transducer.

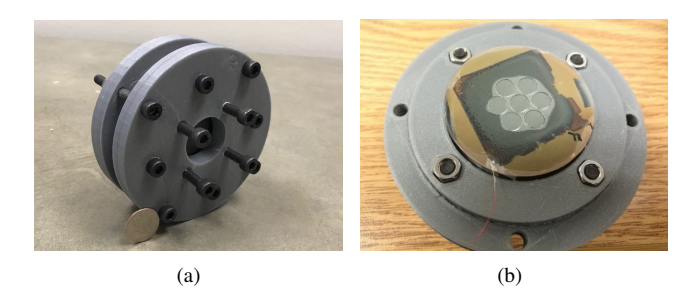


Fig. 3: The assembled transducers: (a) 3D-printed transducer; (b) an assembled transducer with rGO membrane.

about 400 nm (or 0.4 μ m) with a minimum ultimate tensile strength (UTS) of 191 MPa. The strength and thinness of the membrane make it well suited for ultrasound applications. In comparison, pure graphene, the strongest material ever discovered, has a UTS of 130 GPa, but it is extremely brittle. With a smaller gap size (the thickness of spacers), a minor movement of the membrane causes a larger signal variation, which generates a stronger output signal. For the transmitter (or speaker), the electrical signal and the inverse of the signal are sent to the two electrodes separately. According to the Coulomb's law, the voltage changes on the electrodes result in mechanical movements of the membrane, which further trigger the mechanic movements of air according to Eq. (3). The air movements are then transformed into acoustic waves that penetrate the electrodes and travel through the air. The receiver (or microphone) works in a reverse order. The overall cost of an rGO transducer prototype is around \$10, which can be further reduced during mass production.

C. Amplifier Design

The signals directly captured from the membrane vibration are extremely weak signals, which require amplification for

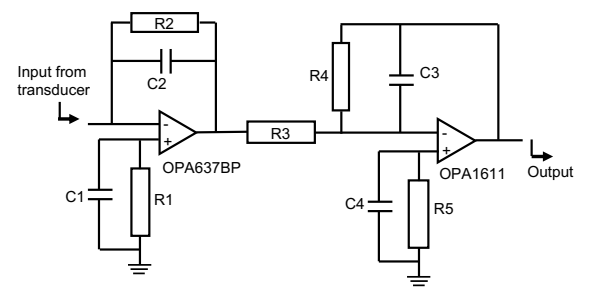


Fig. 4: The schematic diagram of LNA circuit (C1 - C4 are capacitors, and R1 - R5 are resistors).

further signal processing. URadio incorporates two types of amplifiers including a power amplifier (PA) at the transmitter and a low noise amplifier (LNA) at the receiver. The use of LNA is because the received signal at the receiver is particularly susceptible to noise.

At the transmitter, we choose a commercial power amplifier with an operational frequency ranging from 50 kHz to 1.2 MHz and a voltage gain of 30 dB with a maximum voltage of 30 V. The LNA at the receiver requires an extremely low noise figure (< 13 dB) to limit the noise impact. It also requires a broad operational bandwidth (at least 100 kHz - 1 MHz) and a high power gain (at least 35 dB), especially when the system performs high-speed data transmission. The COTS amplifiers are usually either too narrow in bandwidth or too high in noise figure. Here, we design our own LNA system. Fig. 4 shows the schematic diagram of the designed circuit. Since the circuit copes with extremely weak electric current (down to 10 μ A), the electronic components in the circuit must be isolated. Therefore, they need to be soldered on a copper board with pins off the ground. Also, self excitation easily occurs in this 2-stage amplifier circuits due to the high gain (i.e., 30 dB or equivalent to 1,000× gain). To suppress self excitation, a customizable small capacitor (i.e., C2 in Fig. 4) is used to connect the input and the output of the first-stage amplifier. As a result, it raises the self-exciting frequency of this circuit to a much higher frequency (>10 MHz), thereby effectively suppressing self excitation. As shown in Fig. 5, the measured frequency response of this 2-stage amplifier circuit has a broad operational 3 dB bandwidth from DC to 1 MHz.

D. Wideband Ultrasonic OFDM Communication System

At the transmitter side, we use a Keysight 33512B waveform generator to produce arbitrary waveform signals formulated

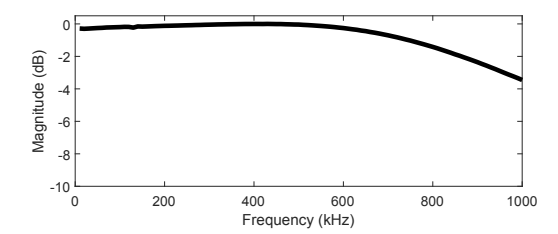


Fig. 5: The frequency response of LNA circuit.

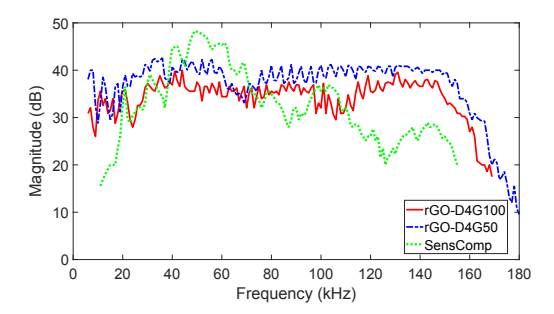


Fig. 6: Frequency response of the end-to-end URadio system with different transmitter-side transducers.

by the software components. At the receiver side, we use both a commercial condenser ultrasound microphone CM16 [19] and our lab-made transducer to capture the ultrasound signals, which will be amplified by the LNA preamplifier. The received signals will be processed by the oscilloscope and subsequently decoded.

To demonstrate the available bandwidth of our system, we measure the end-to-end frequency responses of SensComp and rGO transducers using the commercial ultrasound microphone. Fig. 6 shows that the URadio system with SensComp transducer operates at the range between 20 kHz and 80 kHz with the peak frequency response at around 50 kHz. In contrast, the URadio system with rGO transducers can operate between 10 kHz and 160 kHz, resulting in a much wider bandwidth. The cutoff frequency at 160 kHz is caused by the operating frequency range of CM16 ultrasound microphone, which is between 2 kHz and 180 kHz.

In URadio, due to the available wide bandwidth, OFDM modulation is used to maximize the spectrum utilization. We follow the WiFi protocol by embedding 52 subcarriers into one OFDM symbol. And we utilize linear frequency modulation (LFM) to achieve frame synchronization. Similar to WiFi, long training sequence (LTS) is used to achieve fine-grained time synchronization. Carrier Frequency Offset (CFO) correlation is applied to correct the distortion of the baseband signal. Then, phase error estimation and channel estimation are performed to estimate the channel response and mitigate the channel distortion, which makes the system adaptive to different types of channel conditions. The structure of our OFDM-based frame is presented in Fig. 7. Next, we explain the details of key software components of URadio.

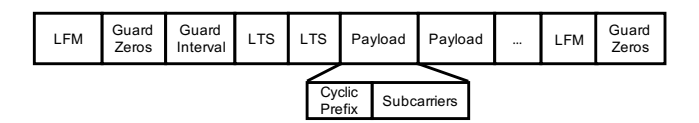


Fig. 7: The structure of an OFDM-based frame.

1) Synchronization: Synchronization in URadio is achieved via two steps. First, the receiver identifies every incoming packet based on coarse synchronization, which relies on an LFM signal located at the head of each packet. Once a packet is detected, a fine synchronization will be processed by the receiver to determine the exact starting time of a packet payload. The LFM signal, known as a chirp signal, has been implemented in radars because of its superior autocorrelation performance and its robustness against additive noises [20]. The LFM signal can be described as follows:

$$S(t) = A \cdot \cos(2\pi t (f_0 + k/2 * t) + \phi), \tag{4}$$

where A is the amplitude, f_0 is the starting frequency, k is the rate of frequency change, and ϕ is the phase. The correlation peaks of the received signal with a local copy of LFM indicates the start of the arriving data sequence. The configurations of f_0 and k are determined by the bandwidth of the ultrasonic communication, which is illustrated below.

After the frame synchronization and downconversion, we use a cross-correlator to search for the 64-sample LTS in the preamble to achieve a fine synchronization. An LTS preamble consists of a sequence of {-1, 1}. Fig. 7 shows two successive LTS used in an OFDM frame. The two LTS preambles are used to precisely locate the start of a packet payload, marking the boundary of each OFDM frame fed into the FFT module.

2) Channel Estimation: Ultrasonic communications over the air are greatly affected by frequency selectivity and multipath fading of an ultrasonic channel. In URadio, LTS is used to estimate the channel impulse response (CIR) and compensate for the channel distortion, in order to turn the frequency-selective channel into a flat channel. During the demodulation, the LTS preambles at the beginning of each package that are known by the receiver are used to correct the phase and amplitude of the received OFDM signals. Thus, the channel estimation H_{est} can be expressed as:

$$H_{est} = LTS \cdot (LTS_1' + LTS_2')/2, \tag{5}$$

where LTS_1' and LTS_2' are the FFT results of the first and second LTS of the received signal, and LTS is a known LTS copy. Because of the relatively stable channel conditions in the high-frequency acoustic spectrum, we compute the average of estimated channels across multiple packages to further improve the estimation accuracy, which helps boost the signal decoding performance.

3) Bandwidth Selection: The operational bandwidth of this OFDM communication system is restricted by two factors: the transducers' resonant frequency and the orthogonality of the carrier signals. As a rule of thumb, the operational bandwidth should be centered around the transducers' resonant frequency to achieve the widest available bandwidth. In URadio, we

¹End-to-end frequency response measures the frequency response of the entire system including circuits and transducers.

use correlation demodulator to achieve downconversion at the receiver side. Our experiments show that, when the carrier frequency f_c is not far greater than the bandwidth², strict orthogonal condition is required for the correlation demodulator to operate properly [21]. Otherwise, the non-orthogonality in the carrier signals will result in significant inter carrier interference (ICI) that increases the bit error rates. The orthogonal condition can be mathematically described as follows:

$$\int_0^{T_s} \cos(2\pi f_c t) \sin(2\pi f_c t) dt = 0, \tag{6}$$

where $T_s = 1/BW$ is the duration of one symbol, and BW is the bandwidth. Via simple derivation from Eq. (6), we can get: $sin^2(2\pi f_c T_s) = sin^2(2\pi f_c/BW) = 0$. Therefore, to maintain such an orthogonality, carrier frequency has to be an integer multiple of a half bandwidth:

$$\frac{f_c}{BW} = \frac{n}{2},\tag{7}$$

where $n \in \mathbb{Z}$ and $n \geq 1$. Let f_h and f_l donate the high and low cutoff frequency of a symbol. Then, $f_c = (f_h + f_l)/2$, $BW = f_h - f_l$. Therefore, Eq. (7) can be further expressed as:

$$f_h = \frac{n+1}{n-1} f_l. {8}$$

Eq. (8) implies that the bandwidth (or the difference between f_h and f_l) is inversely proportional to n, and $n \ge 1$. Thus, we choose n = 2, $f_h = 180$ kHz, $f_l = 60$ kHz with a bandwidth of 120 kHz for the URadio system with our labmade rGO transducer.

E. Serving Multiple Receivers in the Presence of Interference

The current design of the URadio system supports one transmitter-receiver pair. However, the system design can be further extended into a multi-receiver scenario, in which one URadio transmitter can exchange data with multiple URadio receivers using ultrasound. In this case, the transmitter transducer embodies multiple membranes with a spherical shape as shown in Fig. 8, such that the signals can reach multiple receivers along different directions. In order to avoid being exposed to eavesdropping attacks, we configure the new URadio transmitter to only transmit to one receiver at one time. Through multiple rounds of transmission, the messages can be delivered to multiple receivers safely.

The high-frequency acoustic spectrum is mostly clear of environmental noise [22]. As a result, the environmental noise has a minimal impact on the ultrasonic communication performance. However, if some objects block the LoS path between the transmitter and receiver, the message delivery performance will be impaired. As mentioned previously in our threat model (cf. Section II-B), the obstruction of the LoS path can be easily detected by the communicating parties, who can send security alerts to the users. Moreover, just like any other communication systems, URadio can adopt retransmission routines at the upper layer to mitigate the

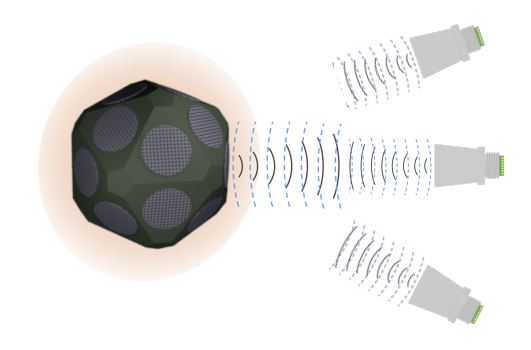


Fig. 8: The design of Tx transducer to serve multiple receivers.

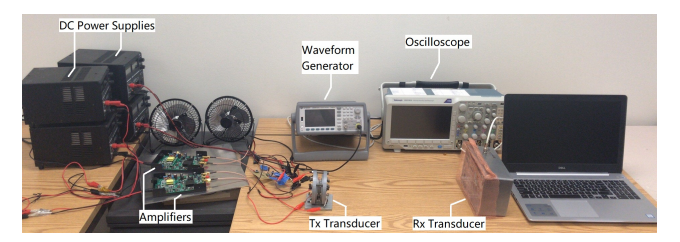


Fig. 9: An illustration of the benchtop experimental setup.

impact of interference caused by the blocking of the LoS path. We leave the upper-layer communication design of URadio as our future work.

IV. EVALUATION

In this section, we conduct comprehensive experiments to evaluate the performance of URadio system. Specifically, we design and perform the experiments to measure URadio's communication and security performance in a lab environment.

A. Experimental Setup

Fig. 9 presents the experimental arrangement for this ultrasonic communication system. The data is processed and modulated by MATLAB programs that run on a laptop before sending to a Keysight 33500B waveform generator through a general purpose interface bus (GPIB). The signals from the waveform generator are amplified by two GWBP-AMP-X75 Power Amplifiers. The amplified signals are then transmitted by the ultrasonic transducer. After travelling through the air, the air-coupled ultrasonic signals are captured by the receiving ultrasonic transducer (i.e., the commercial ultrasound microphone CM16) that is connected to the LNA. Finally, the received signals are digitized by the oscilloscope and sent back to the laptop for post-processing via an Ethernet cable. Unless otherwise specified, all of the experiments are conducted in a laboratory environment with a size of 30 ft \times 30 ft or a long corridor outside of the lab.

B. Communication Capability

We conduct the experiments in an indoor lab environment with no detectable ultrasonic background noise. The transmitter and receiver exchange ultrasonic signals over an LoS link. Four different baseband modulation schemes, i.e., BPSK, QPSK, 16-QAM, and 64-QAM, are used to modulate the OFDM subcarrier signals that range from 45 to 65 kHz in the

²In WiFi systems, the carrier frequency (e.g., 2.4 GHz) is far greater than the channel bandwidth.

Transducers	Mod Type	f_c (kHz)	BandWidth (kHz)	Data Rate (kbps)	Range (cm)	Admissible SNR (dB)	BER	
SensComp	BPSK		20	20	2,090	9.2		
	QPSK	50		40	1,640	11.2	< 10 ⁻⁴	
	16QAM			80	1,200	16.1		
	64QAM			120	620	20.8		
rGO-D4G100	BPSK	120	120	120	95	10.7		
	QPSK		80	160	91	13.4	< 10 ⁻⁴	
	16QAM		60	240	78	18.3	< 10	
	64QAM		60	360	58	20.6		
rGO-D4G50	BPSK		120	120	114	13.3		
	QPSK	120	80	160	98	14.6	< 10 ⁻⁴	
	16QAM		60	240	91	19.6	< 10	
	64QAM		60	360	81	21.1		

TABLE I: URadio communication performance.

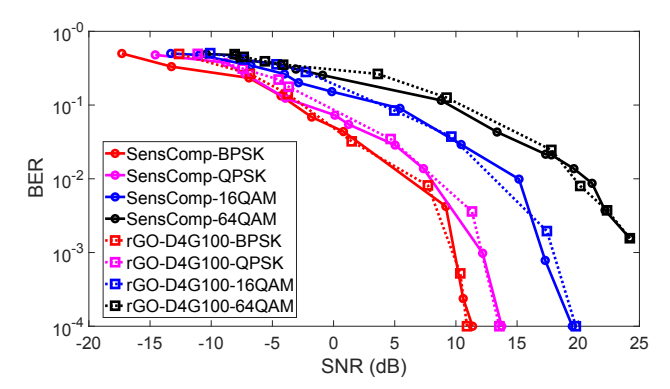


Fig. 10: BER performance of different transducers using different modulation schemes.

URadio system with SensComp transducers, or cover from 60 to 180 kHz in the URadio system with the rGO transducers.

Our first experiment evaluates and compares the performance metrics such as bandwidth, data rate, transmission range, SNR, bit error rate (BER) of all the four modulation schemes using SensComp, rGO-D4G100, and rGO-D4G50 ultrasonic transducers. The BER performance is measured at a fixed communication range (1 meter for SensComp, 15 cm for lab-made transducers) with a proper transmission power. Each 140-Byte packet signal is transmitted 10 times. Fig. 10 shows the BER performance of URadio equipped with SensComp and rGO transducers. The URadio system with rGO transducers can achieve 10⁻⁴ BER at 13 dB SNR using QPSK, and there is a considerable performance gap between systems using QPSK and 16-QAM. The result demonstrates that rGO transducers are capable of operating under a low-SNR environment.

Table I lists the achievable data rate and maximum transmission range using our current instruments with non-detectable BER (i.e., < 10⁻⁴), which shows that URadio achieves a high date rate of 160 kbps, 240 kbps, and 360 kbps while using the lab-made rGO transducers with QPSK, 16-QAM, and 64-QAM, respectively. Also, URadio with rGO-D4G50 transducer achieves a slightly longer communication range than URadio with rGO-D4G100 transducer, due to the power boost brought by a smaller gap size. The results indicate URadio's wide bandwidth communication enables higher speed data rate; meanwhile, URadio can also achieve long range

communication when using SensComp transducers with BPSK modulation. Particularly, the maximum effective transmission range reaches 20.9 m. Given the experimental results, URadio with SensComp can be used for long range applications which do not have a high demand on the transmission data rate, e.g., remote control and sensing. Conversely, URadio with rGO transducers can be used for short range and high data rate applications, e.g., face-to-face file transfer and video streaming.

It is noteworthy that URadio's current communication data rate and distance are limited by the receiver's operating frequency band (2 kHz–180 kHz). Moreover, when the amplifier's output power (0.54 Watts) increases which yields a larger transmission power, URadio will achieve a longer communication range. Hence, URadio's performance can be improved by applying higher-power amplifiers and better acoustic engineering at the receiver end, which we leave for future work.

C. Image Transmission Through Ultrasound

In the second experiment, we evaluate the image transmission performance to validate the high bandwidth transmission capability of the URadio system using rGO membrane. We transform a 512 × 512 pixels bmp format Lena image with 8 bit grey scale into bits, and use the URadio system to carry out image transmission at different transmission ranges. The entire transmission process takes around 900 ms using 16-QAM at a data rate of 240 kbps, showing that URadio is capable of initiating large data transfer that is very useful for a wide variety of smart home applications. Fig. 11 shows the received Lena pictures across different communication distances, the quality of which degrades with increasing distances.

D. Security Evaluation

Ultrasonic signal transmits efficiently over an LoS link, and any angular deviation may result in a significant loss of SNR, which is also the reason why URadio can effectively counter eavesdropping attacks. In this section, we evaluate the performance of URadio under eavesdropping attacks in a long corridor without any obstacles, which emulates a LoS communication scenario. We also conduct the experiments in a laboratory environment with multiple sets of furniture including desks, chairs, and monitor screens, which is similar









Fig. 11: Received Lena pictures of URadio-rGO-D4G50 using 16-QAM with different distances between Alice and Bob: (a) distance = 90 cm, SNR = 18.8 dB; (b) distance = 100 cm, SNR = 15.4 dB; (c) distance = 120 cm, SNR = 10.86 dB; (d) distance = 150 cm, SNR = 3.9 dB.

to a real-world smart home scenario. Then, we evaluate the impact of jamming attacks. Note that in the following experiments, the SensComp transducer operates at the frequency range between 40 kHz and 60 kHz, while the rGO-D4G100 transducer operates at the range of 90 kHz and 150 kHz, both using BPSK modulation unless otherwise specified.

Eavesdropping attack evaluation in a corridor environment. To reduce the impact of multi-paths, we conduct the experiments in an open corridor without any obstacles along the transmission path. Alice and Bob are communicating using the URadio system, while Eve is listening on their private communications. The URadio system assembled with a SensComp is used to test the relationship among different eavesdropping angles, SNR, and BER with different distances between Alice and Eve in the open corridor scenario. The result is presented in Fig. 12. Fig. 12(b) shows that: an eavesdropping angle γ as small as 5° will result in an SNR loss of at least 5 dB at Eve's receiver. Moreover, a 10° angular deviation can cause an SNR dip of more than 20 dB, 15 dB, and 10 dB with a distance of 5 m, 3 m, and 1 m, respectively.

Fig. 13 shows BER performance of eavesdroppers with different eavesdropping angles and different modulation types. For all four modulation types, the BER reaches 50% even with a 15° angular deviation (i.e., γ) at the distance of 5 meters. Notably, higher order modulation schemes are more secure against eavesdroppers, with which the BER performance degrades dramatically when there is only a slight angular deviation. These results indicate that eavesdropping on URadio data transfer will suffer from a bad channel quality, which results in an extremely low eavesdropping accuracy.

Eavesdropping attack evaluation in a multi-path indoor environment. To measure the multi-path effects, we evaluate and compare the eavesdropping attack between Alice and Eve with four modulation types in a small office. The URadio system is assembled with a SensComp or rGO-D4G100. For simplicity, we demonstrate the SNR and BER performance of an eavesdropper when eavesdropping QPSK and 16QAM communications in Fig. 14. The results show that the URadio communication can be eavesdropped at a wider angle compared with the open corridor scenario due to the reflected signal gain introduced by multi-paths. However,

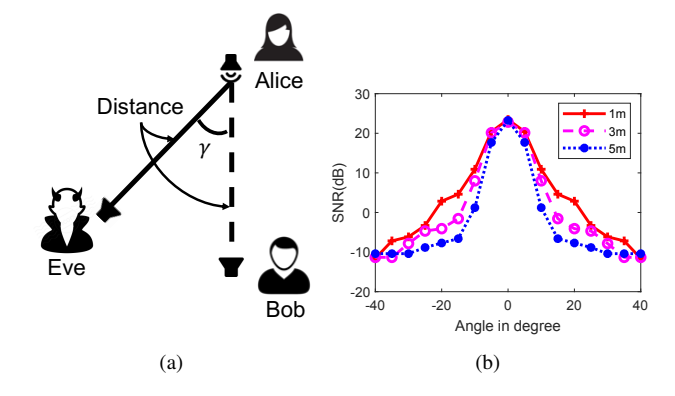


Fig. 12: Eavesdropping attacks evaluation: (a) eavesdropping attack experimental setup; (b) SNR of Eve with different eavesdropping angles and distances using BPSK in an open corridor scenario.

higher order modulation schemes remain more secure against eavesdroppers.

It is worth-noting that: the URadio with rGO-D4G100 demonstrates much better security than URadio with SensComp, i.e., the BER reaches 50% with a 30° angular deviation for URadio-rGO-D4G100 as opposed to a 40° angular deviation for URadio-SensComp. The results indicate that, even in a small indoor multi-path environment, it is difficult to eavesdrop on URadio data transfer, given the directionality of high-frequency ultrasonic communication.

Jamming attack evaluation. Next, we evaluate the jamming resilience performance of URadio system (equipped with SensComp transducers) by setting up an experiment as shown in Fig. 15. We let Eve continuously transmit an ultrasonic jamming signal to Bob, while Bob is receiving benign signals from Alice. Alice is positioned 5 meters away from Bob; Eve is at different positions on the vertical bisector pointing to Bob. The jamming signal is a band-limited Gaussian white noise with its power equal to the source power sent by Alice and its bandwidth covering the entire frequency range of SensComp (i.e., 40 kHz - 60 kHz). The result is shown in Fig. 15, which indicates that jamming attack can only effectively reduce the SNR of received signal by at most 3 dB when the distance

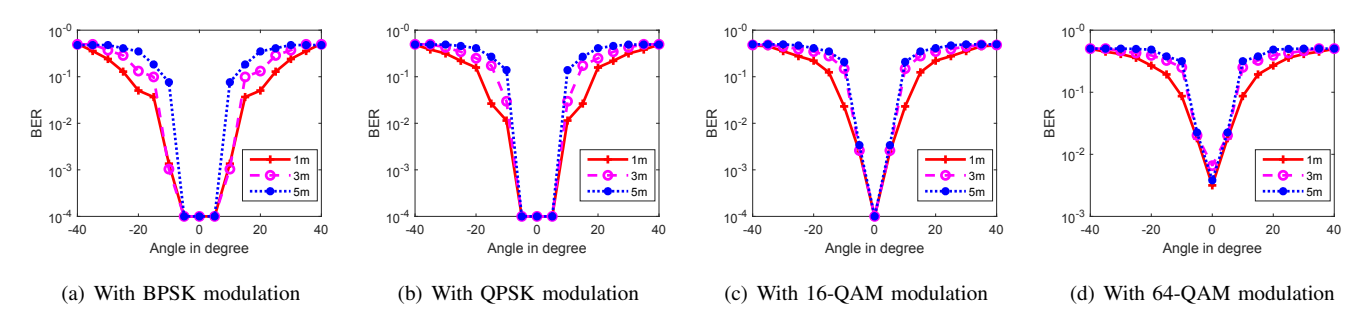


Fig. 13: BER performance of an eavesdropper in a corridor environment.

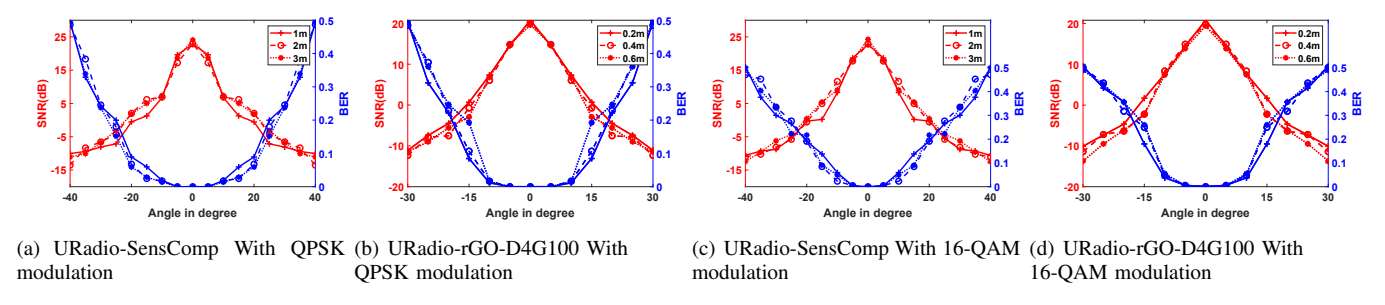


Fig. 14: SNR & BER performance of an eavesdropper in a multi-path indoor environment.

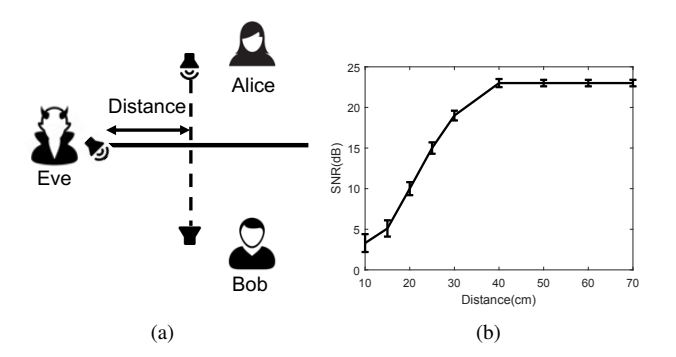


Fig. 15: Eve launches jamming attack to disrupt the communication between Alice and Bob: (a) jamming attack experimental setup; (b) SNR of Bob for the benign communicataion under attack.

between the attacker and communicating parties is very close (i.e., less than 30 cm), demonstrating the jamming resilience of the URadio system.

Summary. Due to the directionality of ultrasound, the message between the transmitter and receiver is delivered through a direct LoS path. As a result, in order to eavesdrop the communication with a satisfactory quality, the attacker has to be residing very close to the LoS path, i.e., less than 5° angular deviation from LoS. Meanwhile, for a successful ultrasonic jamming attack, the adversary has to be very close to the transmitter or receiver (less than 30 cm). As opposed to the relaxed requirements in the RF-based attacks, these strict requirements on the relative positions of the adversaries can lead to their exposure. Therefore, the URadio system is more secure and resilient than its RF counterparts.

E. Comparing with State-of-the-Art

Table II compares URadio with other state-of-the-art airborne ultrasonic communication systems in terms of their maximum error-free transmission range, maximum data rate, power consumptions, and other system characteristics. As is shown in Table II, when using SensComp transducers for data communication, URadio achieves a longer transmission range. Using rGO transducers, URadio significantly improves the data rate at a short range. Therefore, if the data throughput is considered as the first priority, our lab-made transducers with broader bandwidth should be used. On the other hand, if the transmission range is considered as the top priority, the SensComp transducer could be employed.

Compared with previous work that primarily considers a small amount of data exchange, URadio can handle file transfer of a large size. The high-speed communication capability integrated with security features makes URadio particularly suited for secure smart home applications. Note that Jiang et al.'s system [24] can also achieve high-speed ultrasonic communication. However, their membrane is twice thicker (0.8 μ m vs. 0.4 μ m) and only supports a lower-order modulation, i.e., 16-QAM. Therefore, it is expected that, with a higher upper limit on the communication capability, URadio can further improve the transmission data rate and range by expanding the bandwidth and increasing the transmission power.

Regarding the power consumption, the comparison results in Table II indicate that URadio requires a lower power consumption than BackDoor [6]. Even though U-Wear [5] consumes the least power, U-Wear only supports a very low data rate. Most of the existing work does not present the power consumption of the systems, including the ultrasonic system

, ,	,					
Systems	Mod. Type	Data Rate	Range	Power	Transducer Hardware	Transducer Cost
U-Wear [5]	16QAM-OFDM	2.76K	N/A	0.02	COTS	N/A
BackDoor [6]	AM	4K	100	2	COTS	\$4
Chirp [7]	chirp	16	2,500	N/A	COTS	N/A
Multi-Tone [8]	MFSK	800	N/A	N/A	COTS	N/A
Short-Range [23]	QPSK	200K	1,200	N/A	COTS	N/A
Indoor [24]	16QAM-OFDM	800K	70	N/A	Custom-Made	N/A

20K

360K

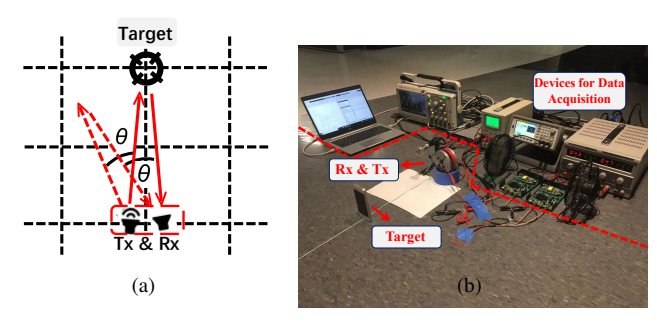
TABLE II: System comparison (data rate: *bps*, range: *cm*, power: *watt*; N/A means the specific system characteristics are not provided by the respective work).

URadio-SC is the URadio system with SensComp transducers. URadio-rGO-D4G50 is the URadio system with rGO transducers.

2.090

0.54

0.54



BPSK-OFDM

64QAM-OFDM

URadio-SC

URadio-rGO-D4G50

Fig. 16: Experimental setup for the object localization application: (a) experimental platform consisting of the target object at different locations and the transmitter-receiver pair (placed at (0,0)) with different facing angles θ ; (b) instruments used in the real experiments.

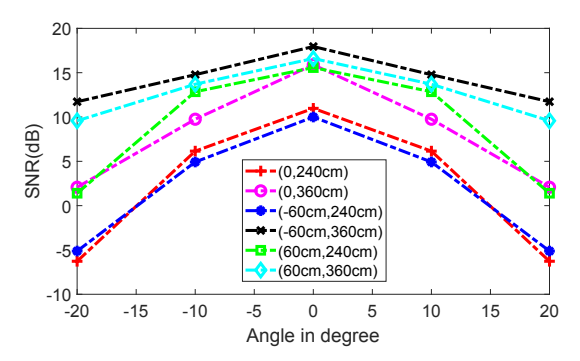
with a comparable data date in [24]. Since URadio has a much thinner membrane than others, we believe that with a comparable power usage, URadio can achieve a higher data rate communication. In terms of the hardware usage, URadio supports both COTS and custom-made transducers with a reasonable hardware cost, while most of the existing systems use a COTS transducer without specifying the hardware costs.

V. SECURE OBJECT LOCALIZATION APPLICATION USING URADIO

This section presents an application of URadio for object localization. Object localization has been a popular application used to recognize, model, and predict daily activities in a smart home environment [25]. RF-based object localization has been investigated [26], but such scheme is subject to various RF-based attacks [27], which affect the localization accuracy. Because of URadio's security and directionality properties, by analyzing the reflected ultrasound signals from a particular object, we can precisely and securely localize the object.

Experimental setup and range detection. To evaluate the secure object localization enabled by URadio, we set up an experimental platform as shown in Fig. 16. An iPhone-5s (123.8 mm×58.6 mm ×7.6 mm) as the target object is placed at the pre-defined locations for object localization. The ultrasound transmitter and receiver (which we call *URadio pair*) are placed side-by-side.

We first point the transmitter and receiver to the target object for acquiring the best SNR, denoted as the *ground truth*. In order to detect the direction of the target object, we adjust the URadio pair's facing angles as shown in Fig. 16(a). When



COTS

Custom-Made

\$25

~\$10

Fig. 17: Secure object localization: received SNR performance of URadio-Senscomp with a target object at different locations (in legend) with different facing angles (transmitter-receiver pair is placed at (0,0)).

the receiver detects a signal with the highest SNR, the facing direction of the transmitter corresponds to the direction of the target object. Next, we measure the maximum monitoring area using the SensComp as the transmitter. The target object is placed at 6 different locations, and the maximum reflected path length is around 7 meters for the location (± 60 cm, 360 cm). The received SNR performance in Fig. 17 demonstrates the excellent directionality of URadio, in which a slight facing angle of 10° will result in an SNR loss of at least 5 dB. As a result, we will be able to localize the target object reliably in a 14 $m \times 14$ m area with the URadio pair at its center.

Object localization performance comparison. To measure and compare the localization errors with SensComp and rGO based URadio systems, we test the direction estimation performance of URadio system assembled with different transmitters in an open corridor scenario. Fig. 18 shows the received SNR & BER performance of reflected signals by a target object. The results demonstrate that rGO-D4G100 achieves a much better direction estimation than the commercial SensComp, in which a small facing angle of 5° will result in an SNR loss of at least 10 dB for rGO-D4G100 and a mere 15° facing angular deviation can bring BER up by 50%.

Given a known reflected path length, leveraging the accurate direction estimation, we can derive the target object's location. Specifically, the facing angle θ with the highest received SNR will be determined as the direction to the target object. Here, we define 90% of the highest received SNR as ambiguous SNR values, which correspond to ambiguous object directions, defined as ambiguous angle range. We compute the average

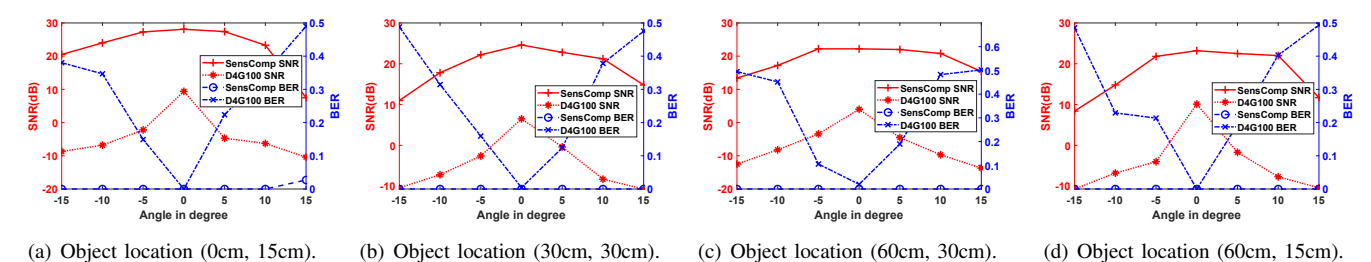


Fig. 18: Received SNR & BER performance of reflected signals by an object for different transmitters with different facing angles (transmitter-receiver pair is at (0,0)).

TABLE III: URadio object localization performance comparison.

Target		ingle Range (°)	Loc Error (cm)		
	URadio-SC	URadio-rGO	URadio-SC	URadio-rGO	
(-30, 15)	(-7.2, 7.2)	(-1.2, 1.2)	(-1.64, -3.87)	(-0.31, -0.63)	
(-30, 30)	(-3, 4.5)	(-1.5, 2.1)	(-1.88, -2.02)	(-0.92, -0.95)	
(0, 30)	(-3.3, 3.9)	(-1.5, 1.8)	(-1.87, -0.06)	(-0.85, -0.02)	
(30, 30)	(-6.3, 8.4)	(-1.8, 1.5)	(-4.08, +3.59)	(-0.87, +0.85)	
(30, 15)	(-5.1, 10.5)	(-1.2, 1.5)	(-2.31, +3.93)	(-0.36, +0.70)	

URadio-SC: URadio system with SensComp URadio-rGO: URadio system with rGO-D4G100

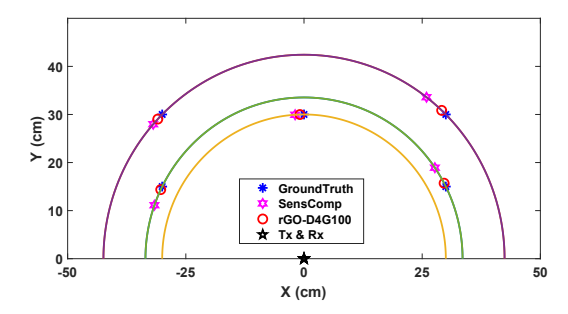


Fig. 19: Object localization performance for different transmitters (transmitter-receiver pair is at (0,0)).

estimated angle deviation, with which we can derive the estimated location based on the known distance. Note that the SNR distribution is measured and averaged to ensure the robustness and accuracy of experiments. The localization error is calculated with respect to the X and Y coordinates.

Fig. 19 presents the localization ground truth, the estimated location by URadio-SensComp system, and the estimated one by URadio-rGO-D4G100 system. The results demonstrate that the lab-made rGO-D4G100 achieves less localization error compared with the commercial SensComp qualitatively. We provide the localization errors for a set of target locations in Table III, which indicates that URadio-rGO-D4G100 can achieve less than 1 cm localization error for each dimension in the 85 cm \times 85 cm area. The result also demonstrates that the URadio-rGO-D4G100 outperforms the URadio-SensComp in terms of the accuracy of object localization.

VI. RELATED WORK

Using ultrasound as a carrier to achieve data transmission has long been investigated. The modulated ultrasound has been widely used in underwater communications [28]. Jiang et al. [29] achieve a full-duplex point-to-point ultrasonic transmission with two pairs of transducers, a function generator, and an oscilloscope. U-Wear [5] goes beyond a simple point-to-point transmission scheme by interconnecting

multiple wearable devices using ultrasound. Jiang et al. [30] recently develop a prototype of an indoor ultrasonic communication network with ceiling-mounted transceivers.

Recent studies use ultrasound for sensing, with applications in gesture recognition, health monitoring, and localization. Wang et al. [31] introduce a contact-free gesture recognition system based on ultrasound. Nandakumar et al. [32] use the acoustic wave to track heartbeat by examining periodic wave patterns. Liu et al. [33] leverage audio signals to achieve localization of keystrokes from a single phone behind the keyboard. With wider bandwidth and higher frequency, URadio could potentially improve the accuracy of these emerging sensing applications.

In addition, since ultrasound signals are inaudible, it can be also used as hidden communication for smart home devices, with either benign or malicious purpose. The nonlinear behavior of MEMS microphones has been utilized to achieve data transmission [6]. Zhou et al. enable real-time unobtrusive speaker-microphone data communication using ultrasonic signal [34], without affecting the primary audio-hearing experience of human users. Moreover, ultrasonic signal can be used maliciously to launch inaudible attacks, which pose a threat to smart home security [35]. For example, Zhang et al. [36] show that the adversaries can exploit the microphones' non-linearity to send inaudible ultrasound that forces the microphone to record malicious ultrasonic signals as normal voice commands, thereby hijacking voice assistants. Roy et al. further improve the attack range using an array of ultrasonic transducers [37].

Mechanic components in devices, such as sensors, hard disk read-and-write head, are also susceptible to airborne ultrasonic attack that exploits their mechanical resonant frequency. Bolton et al. launch an ultrasonic attack on mechanic hard disk drive, which can cause physical causality and even OS failures [38]. Researchers achieved a denial-of-service attack and arbitrary manipulation of sensor outputs by injecting well-formed ultrasonic signals with specific frequencies to sensors (i.e., gyroscope, accelerometer, etc) [39]. While these ultrasonic attacks towards smart home devices are devastating, we explore a new direction on securing the smart home using ultrasound communication.

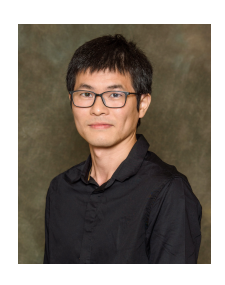
VII. CONCLUSION

In this paper, we introduced rGO transducers for smart home ultrasonic communications for the first time. We presented URadio, a secure and high data rate ultrasonic communication system. URadio achieves 20 kbps data rate with a communication range of 20.9 meters with COTS transducers, while the new rGO transducers increase the achievable data rate to 360 kbps with an attainable range of 81 cm. The communication range of rGO transducers can be further improved by power amplifier. We have built a prototype of URadio using lab-made rGO transducers and evaluated its performance in different scenarios. Experimental results show that URadio offers much higher data rate and larger communication range than its existing counterparts. We also demonstrated its versatility in smart home through showcasing its secure applications such as image transmission, jamming-resilient communication, antieavesdropping communication, and fine-grained (centimeterlevel) indoor localization. Breaking out of the RF realm, URadio offers a new communication system that could potentially enhance the reliability and security of smart home applications.

REFERENCES

- Q. Yan, H. Zeng, T. Jiang, M. Li, W. Lou, and Y. T. Hou, "Mimobased jamming resilient communication in wireless networks," in *Proc.* of *INFOCOM*, 2014, pp. 2697–2706.
- [2] D. Kapetanovic, G. Zheng, and F. Rusek, "Physical layer security for massive mimo: An overview on passive eavesdropping and active attacks," *IEEE Communications Magazine*, vol. 53, no. 6, pp. 21–27, 2015.
- [3] C. Pöpper, N. O. Tippenhauer, B. Danev, and S. Capkun, "Investigation of signal and message manipulations on the wireless channel," in European Symposium on Research in Computer Security, 2011.
- [4] D. Schindel and D. Hutchins, "Applications of micromachined capacitance transducers in air-coupled ultrasonics and nondestructive evaluation," *IEEE transactions on ultrasonics, ferroelectrics, and frequency control*, vol. 42, no. 1, pp. 51–58, 1995.
- [5] G. E. Santagati and T. Melodia, "U-wear: Software-defined ultrasonic networking for wearable devices," in *Proc. of MobiSys*, 2015, pp. 241– 256.
- [6] N. Roy, H. Hassanieh, and R. Roy Choudhury, "Backdoor: Making microphones hear inaudible sounds," in *Proc. of MobiSys*, 2017, pp. 2–14.
- [7] H. Lee, T. H. Kim, J. W. Choi, and S. Choi, "Chirp signal-based aerial acoustic communication for smart devices," in *Proc. of INFOCOM*, 2015
- [8] T. Hosman, M. Yeary, J. K. Antonio, and B. Hobbs, "Multi-tone fsk for ultrasonic communication," in *IEEE Instrumentation and Measurement Technology Conference (I2MTC)*, 2010, pp. 1424–1429.
- [9] "Silverpush," http://www.silverpush.co/, Accessed on Jan. 2, 2020.
- [10] Q. Zhou, J. Zheng, S. Onishi, M. Crommie, and A. K. Zettl, "Graphene electrostatic microphone and ultrasonic radio," *Proceedings of the National Academy of Sciences*, vol. 112, no. 29, pp. 8942–8946, 2015.
- [11] G. Eda, G. Fanchini, and M. Chhowalla, "Large-area ultrathin films of reduced graphene oxide as a transparent and flexible electronic material," *Nature nanotechnology*, vol. 3, no. 5, p. 270, 2008.
- [12] D. A. Dikin, S. Stankovich, E. J. Zimney, R. D. Piner, G. H. Dommett, G. Evmenenko, S. T. Nguyen, and R. S. Ruoff, "Preparation and characterization of graphene oxide paper," *Nature*, vol. 448, no. 7152, p. 457, 2007.
- [13] A. Udall, "How ultrasound sensing makes nest displays more accessible," https://blog.google/products/google-nest/ultrasound-sensing/, Dec. 2019. Accessed on Nov. 4, 2021.
- [14] S. Hollister, "Amazon will let you teach alexa to recognize and respond to sounds and detect occupancy," https://www.theverge.com/2021/9/28/ 22696536/amazon-alexa-echo-recognize-sounds-teach-ai, Sep. 2021. Accessed on Nov. 4, 2021.
- [15] T. F. Embleton, "Tutorial on sound propagation outdoors," The Journal of the Acoustical Society of America, vol. 100, no. 1, pp. 31–48, 1996.
- [16] K. Attenborough, "Review of ground effects on outdoor sound propagation from continuous broadband sources," *Applied acoustics*, vol. 24, no. 4, pp. 289–319, 1988.

- [17] N. Komninos, E. Philippou, and A. Pitsillides, "Survey in smart grid and smart home security: Issues, challenges and countermeasures," *IEEE Communications Surveys & Tutorials*, vol. 16, no. 4, pp. 1933–1954, 2014.
- [18] Senscomp. [Online]. Available: http://www.senscomp.com/pdfs/ series-600-instr-grade-ultrasonic-sensor-spec.pdf
- [19] "Condenser ultrasound microphone cm16/cmpa," http://www.avisoft. com/ultrasound-microphones/cm16-cmpa/, Accessed on Jan. 2, 2020.
- [20] M. Soumekh, Synthetic aperture radar signal processing. New York: Wiley, 1999, vol. 7.
- [21] A. R. Bahai, B. R. Saltzberg, and M. Ergen, Multi-carrier digital communications: theory and applications of OFDM. Springer Science & Business Media, 2004.
- [22] "Let's talk sound frequencies," https://www.attune.com.au/2020/02/12/lets-talk-sound-frequencies/, Accessed on Nov. 2, 2021.
- [23] C. Li, D. A. Hutchins, and R. J. Green, "Short-range ultrasonic communications in air using quadrature modulation," *IEEE transactions on ultrasonics, ferroelectrics, and frequency control*, vol. 56, no. 10, 2009.
- [24] W. Jiang and W. M. Wright, "Indoor airborne ultrasonic wireless communication using ofdm methods," *IEEE transactions on ultrasonics*, ferroelectrics, and frequency control, vol. 64, no. 9, pp. 1345–1353, 2017.
- [25] D. Fortin-Simard, K. Bouchard, S. Gaboury, B. Bouchard, and A. Bouzouane, "Accurate passive rfid localization system for smart homes," in 2012 IEEE 3rd International Conference on Networked Embedded Systems for Every Application (NESEA), 2012, pp. 1–8.
- [26] D. Zhang, J. Ma, Q. Chen, and L. M. Ni, "An rf-based system for tracking transceiver-free objects," in *Fifth Annual IEEE International Conference on Pervasive Computing and Communications (PerCom'07)*. IEEE, 2007, pp. 135–144.
- [27] P. Yang, W. Wu, M. Moniri, and C. C. Chibelushi, "Efficient object localization using sparsely distributed passive rfid tags," *IEEE transactions* on industrial electronics, vol. 60, no. 12, pp. 5914–5924, 2012.
- [28] T.-H. Won and S.-J. Park, "Design and implementation of an omnidirectional underwater acoustic micro-modem based on a low-power micro-controller unit," Sensors, vol. 12, no. 2, pp. 2309–2323, 2012.
- [29] W. Jiang and W. M. Wright, "Full-duplex airborne ultrasonic data communication using a pilot-aided qam-ofdm modulation scheme," *IEEE transactions on ultrasonics, ferroelectrics, and frequency control*, vol. 63, no. 8, pp. 1177–1185, 2016.
- [30] —, "An indoor airborne ultrasonic wireless communication network," IEEE Transactions on Ultrasonics, Ferroelectrics, and Frequency Control, vol. 65, no. 8, pp. 1452–1459, 2018.
- [31] Y. Wang, J. Shen, and Y. Zheng, "Push the limit of acoustic gesture recognition," in *IEEE INFOCOM 2020-IEEE Conference on Computer Communications*. IEEE, 2020, pp. 566–575.
- [32] R. Nandakumar, S. Gollakota, and N. Watson, "Contactless sleep apnea detection on smartphones," in *Proceedings of the 13th annual interna*tional conference on mobile systems, applications, and services, 2015, pp. 45–57.
- [33] J. Liu, Y. Wang, G. Kar, Y. Chen, J. Yang, and M. Gruteser, "Snooping keystrokes with mm-level audio ranging on a single phone," in *Proceedings of the 21st Annual International Conference on Mobile Computing and Networking*, 2015, pp. 142–154.
- [34] M. Zhou, Q. Wang, K. Ren, D. Koutsonikolas, L. Su, and Y. Chen, "Dolphin: Real-time hidden acoustic signal capture with smartphones," *IEEE Transactions on Mobile Computing*, 2018.
- [35] Q. Yan, K. Liu, Q. Zhou, H. Guo, and N. Zhang, "Surfingattack: Interactive hidden attack on voice assistants using ultrasonic guided wave," in Network and Distributed Systems Security (NDSS) Symposium, 2020
- [36] G. Zhang, C. Yan, X. Ji, T. Zhang, T. Zhang, and W. Xu, "Dolphinattack: Inaudible voice commands," in *Proc. of CCS*, 2017, pp. 103–117.
- [37] N. Roy, S. Shen, H. Hassanieh, and R. R. Choudhury, "Inaudible voice commands: The long-range attack and defense," in *Proc. of NSDI*, 2018, pp. 547–560.
- [38] C. Bolton, S. Rampazzi, C. Li, A. Kwong, W. Xu, and K. Fu, "Blue note: How intentional acoustic interference damages availability and integrity in hard disk drives and operating systems," in *Proc. of IEEE S&P*, 2018.
- [39] M. Backes, M. Dürmuth, S. Gerling, M. Pinkal, and C. Sporleder, "Acoustic side-channel attacks on printers." in *Proc. of USENIX Security*, 2010.



Qiben Yan (M'15-SM'21) is an Assistant Professor in Department of Computer Science and Engineering of Michigan State University, East Lansing, MI, USA. Prior to joining MSU, he was an Assistant Professor at the University of Nebraska-Lincoln, Lincoln, Nebraska, USA. He received his Ph.D. in Computer Science department from Virginia Tech, an M.S. and a B.S. degree in Electronic Engineering from Fudan University in Shanghai, China. He is a recipient of NSF CRII award in 2016. He received the Best Paper Award from IEEE SECON 2021

and ACM SenSys 2021. His current research interests include wireless communication, blockchain systems, mobile and IoT security, AI security, and big data security and privacy.



Qi Xia received the B.Sc. degree in electrical engineering from Hefei University of Technology, Hefei, China, in 2010, and the M.Sc. degree in electrical engineering from Beijing University of Posts and Telecommunications, in 2014 and another M.Sc degree in Computer Science from University of Nebraska-Lincoln. He is currently pursuing a Ph.D. degree with the Department of Electronic Engineering in University of Texas San Antonio, San Antonio, TX, USA. His research interests include mobile security, acoustic security, and IoT security.



Yuanda Wang received the B.Sc. degree in electrical engineering from the Xi'an Jiaotong University, Xi'an, China, in 2016, and the M.Sc. degree in electrical engineering from North China Electrical Power University, in 2019. He is currently pursuing the Ph.D. degree with the Department of Computer Science and Engineering, Michigan State University, East Lansing, MI, USA. His research interests include mobile security, AI security, and IoT security.



Pan Zhou (S'07–M'14-SM'20) is currently a full professor and PhD advisor with Hubei Engineering Research Center on Big Data Security, School of Cyber Science and Engineering, Huazhong University of Science and Technology (HUST), Wuhan, P.R. China. He received his Ph.D. in the School of Electrical and Computer Engineering at the Georgia Institute of Technology (Georgia Tech) in 2011, Atlanta, USA. He received his B.S. degree in the Advanced Class of HUST, and a M.S. degree in the Department of Electronics and Information En-

gineering from HUST, Wuhan, China, in 2006 and 2008, respectively. He held honorary degree in his bachelor and merit research award of HUST in his master study. He was a senior technical member at Oracle Inc., America, during 2011 to 2013, and worked on Hadoop and distributed storage system for big data analytics at Oracle Cloud Platform. He received the "Rising Star in Science and Technology of HUST" in 2017. He is currently an associate editor of IEEE Transactions on Network Science and Engineering. His current research interest includes: security and privacy, big data analytics, machine learning, and information networks.



Huacheng Zeng (SM'20) received a Ph.D. degree in Computer Engineering from Virginia Tech, Blacksburg, VA. He is currently an Assistant Professor in the Department of Computer Science and Engineering at Michigan State University (MSU), East Lansing, MI. Prior to joining MSU, he was an Assistant Professor of Electrical and Computer Engineering at the University of Louisville, Louisville, KY, and a Senior System Engineer at Marvell Semiconductor, Santa Clara, CA. He is a recipient of the NSF CAREER Award. He received the Best Paper Award

from IEEE SECON 2021 and ACM WUWNet 2014. His research interest is broadly in wireless networking and sensing systems.